Inorg. Chem. **2008**, *47*, 6262−6272

Synthesis, Structural Characterization, and Antiinflammatory Activity of Triethylphosphinegold(I) Sulfanylpropenoates of the Type [$(AuPEt_3)_2$xspa] [H_2xspa = 3-(Aryl)-2-sulfanylpropenoic acid]: an $(H_2O)_6$ Cluster in the Lattice of the Complexes [$(AuPEt_3)_2$xspa]·$3H_2O$

Elena Barreiro,[†] José S. Casas,[†] María D. Couce,[‡] Ángeles Gato,[§] Agustín Sánchez,[†] José Sordo,[*,†] José M. Varela,[†] and Ezequiel M. Vázquez López[‡]

Departamento de Química Inorgánica, Facultade de Farmacia, Universidade de Santiago de Compostela, 15782 Santiago de Compostela, Galicia, Spain, Departamento de Química Inorgánica, Facultade de Ciencias, Universidade de Vigo, 36310 Vigo, Galicia, Spain, and Departamento de Farmacoloxía, Facultade de Farmacia, Universidade de Santiago de Compostela, 15782 Santiago de Compostela, Galicia, Spain

Received February 19, 2008

Gold complexes of the type [$(AuPEt_3)_2$xspa] were prepared by reacting $AuPEt_3Cl$ in basic media with the 3-(aryl)-2-sulfanylpropenoic acids H_2xspa [x = p, Clp, -o-mp, -p-mp, -o-hp, -p-hp, diBr-o-hp, f, t, -o-py; p = 3-phenyl, Clp = 3-(2-chlorophenyl)-, -o-mp = 3-(2-methoxyphenyl)-, -p-mp = 3-(4-methoxyphenyl)-, -o-hp = 3-(2-hydroxyphenyl)-, -p-hp = 3-(4-hydroxyphenyl)-, diBr-o-hp = 3-(3,5- dibromo-2-hydroxyphenyl)-, f = 3-(2-furyl)-, t = 3-(2-thienyl)-, -o-py = 3-(2-pyridyl); spa = 2-sulfanylpropenoato], and 2-cyclopentylidene-2-sulfanylacetic acid (H_2cpa). The complexes were characterized by spectroscopic methods (IR, ^{1}H, ^{13}C and ^{31}P NMR) and mass spectrometry, and the complexes [$(AuPEt_3)_2$pspa]·$3H_2O$, [$(AuPEt_3)_2$-p-hpspa]·$3H_2O$, [$(AuPEt_3)_2$tspa)]·$3H_2O$, and [$(AuPEt_3)_2$-o-hpspa] by X-ray diffractometry. The crystals of the first three complexes contain $(H_2O)_6$ clusters hydrogen bonded to [$(AuPEt_3)_2$xspa]$_2$ dimer units, whereas in the -o-hpspa derivative the hydrogen bonds are between the monomer [$(AuPEt_3)_2$-o-hpspa] units. The antiinflammatory activity of the complexes against plantar edema induced by carrageenan in rats is generally significant, with the values for the o-hpspa and tspa derivatives being particularly high.

Introduction

Rheumatoid arthritis is a disease of unknown origin and is characterized by persistent inflammation and joint swelling, functional disability, and increased mortality. Inflammation occurs first in the synovial membrane that surrounds the joints and then moves into the synovial cavity between the bones. Although no curative therapy exists at present, the disease-modifying rheumatoid arthritis drugs can delay and sometimes cause remission of the disease.

Gold compounds are among these drugs.[1] The molecular basis for their therapeutic effects is not well understood, and although many pathways have been proposed to explain this behavior, the activity is probably a combination of biological effects.[2] For example, gold can replace Zn(II) from a Zn-binding site in the neutrophil collagenase, thus inhibiting the protein,[3] or it can interfere with the homeostasis of the Cu(I) ion by binding to Cu(I)-responsive transcription factors and other Cu(I)-trafficking proteins.[4] Furthermore, gold may also

* To whom correspondence should be addressed. E-mail: qijsordo@usc.es. Tel: +34981528074. Fax: +34981547102.
† Departamento de Química Inorgánica, Facultade de Farmacia, Universidade de Santiago de Compostela.
‡ Universidade de Vigo.
§ Departamento de Farmacoloxía, Facultade de Farmacia, Universidade de Santiago de Compostela.

(1) (a) Messori, L.; Marcon, G. *Met. Ions Biol. Syst.* **2004**, *41*, 279. (b) Eisler, R. *Inflammation Res.* **2003**, *52*, 487. (c) Shaw, C. F., III In *Gold: Progress in Chemistry, Biochemistry and Technology*; Schmidbaur, H., Ed.; J. Wiley & Sons: Chichester, U.K., 1999; p. 260. (d) Fricker, S. P. *Gold Bull.* **1996**, *29*, 53. (e) Parish, R. V.; Cottrill, S. M. *Gold Bull.* **1987**, *20*, 3.
(2) Gunatilleke, S. S.; Barrios, A. M. *J. Med. Chem.* **2006**, *49*, 3933.
(3) Mallya, S. K.; Van Hart, H. E. *J. Biol. Chem.* **1989**, *264*, 1594.
(4) Stoyanov, J. V.; Brown, N. L. *J. Biol. Chem.* **2003**, *278*, 1407.

10.1021/ic800314p CCC: $40.75
Published on Web 06/18/2008

affect the ROS generation,[5] inhibit T-cell proliferation and modulate the immune system,[6] induce mitochondrial membrane permeability,[7] inhibit osteoclast bone resorption,[8] inhibit the activation of NF-κB, a transcription factor responsible for the production of TNF[a] and other key inflammatory cytokines,[9] as well as inhibit the activity of cathepsins, a family of highly homologous, cysteine-dependent enzymes implicated in inflammation and joint destruction.[2]

Gold drugs in clinical use today include the following thiolates, gold(I) sodium thiomalate, gold(I) thioglucose, sodium bis(thiosulfato)gold(I) or sodium thiopropanol sulfonate-S-gold(I), and triethylphosphine (2,3,4,6-tetra-O-acetyl-β-1-D-thiopyranosato-S) gold(I), which is also known as triethylphosphine(tetraacetato thioglucose)gold(I), as [(AuPEt$_3$)tatg], and as auranofin, with the latter compound only administered orally.

Auranofin is a monomeric lipophilic complex that contains[10] a gold(I) center bonded to an S atom (2.29 Å) and a P atom (2.26 Å) in an almost linear environment (S−Au−P: 174°). This compound, despite the strong binding of the thiolate and the phosphine, undergoes a considerable number of ligand exchange reactions.[11,12] The thiolate ligand is rapidly lost in vivo,[11] and this is followed by a slower displacement and concomitant oxidation of the phosphine to Et$_3$PO.

Besides these exchange reactions, a mild oxidation that gave gold clusters and disulfide was recently studied for auranofin and for the equivalent PMe$_3$ derivative.[13] This oxidation process is shown in Scheme 1.

Scheme 1

$$2\,[(AuL)tatg] \longrightarrow \tfrac{1}{2}\,(tatg)_2 + [(AuL)_2(\mu\text{-}tatg)]^+$$

This reaction enabled the synthesis and structural study of the PMe$_3$ derivative, which proved to be [(AuPMe$_3$)$_2$(μ-tatg)]$_2$(NO$_3$)$_2$: a dimer containing Au$_4$ clusters formed through Au−Au interactions between two cationic digold units each containing a AuS$_2$P$_2$ fragment. This Au$_4$ cluster is also present in the oxidation products of other Au(I) phosphine thiolate complexes,[14,15] and the isolated digold units were previously identified[16] in acidic solutions of auranofin.

In a previous study[17] we prepared triphenylphosphine Au(I) derivatives of sulfanylcarboxylates H$_2$L. These complexes [(AuPPh$_3$)$_2$L] are dinuclear and also contain the SAu$_2$P$_2$ fragments but do not dimerize. The sulfanylcarboxylate ligand contains a second donor group, a carboxylate group, which from an electrostatic point of view could play the role of the NO$_3^-$ anion present in the PMe$_3$ auranofin analog. However, in our case[17] this group is coordinated to the metal, thus introducing a significant difference with respect to simple thiolates.

Scheme 2

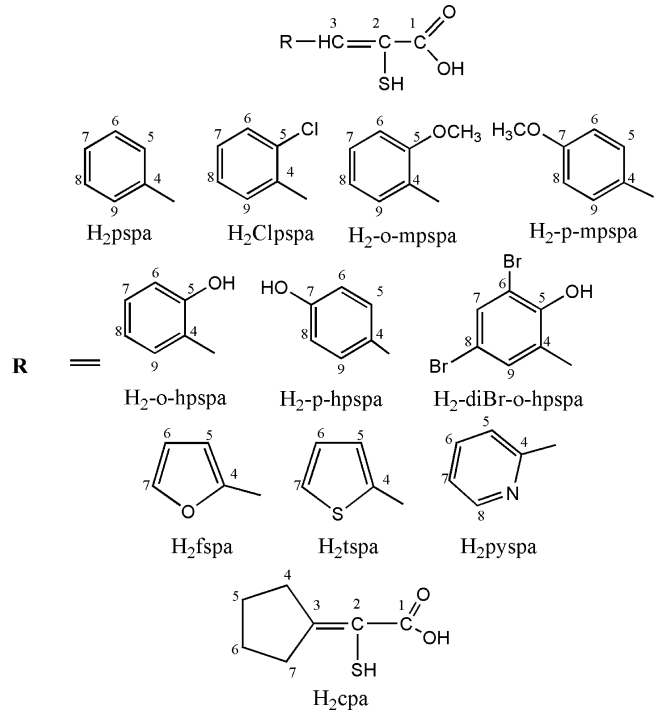

The role of the phosphine also seems to be significant, not only because crystallization of the oxidation product was difficult in auranofin but also because all of the previous structural data on Au$_4$ tetramers from thiolates relates to phosphines such as PMe$_3$, PPh$_3$ or other complex phosphine derivatives but not from PEt$_3$, as highlighted by a search on CSD.[18] Therefore, to gain an insight into the structural chemistry of such species and to investigate the potential therapeutic activity of the resulting complexes, we decided to investigate the reaction of AuPEt$_3$Cl with the 3-(aryl)-2-sulfanylpropenoic acids (H$_2$xspa) and 2-cyclopentylidene-2-sulfanylacetic acid (H$_2$cpa) depicted in Scheme 2 (H$_2$L).

The crystal structures of [(AuPEt$_3$)$_2$pspa]·3H$_2$O (**1**·3H$_2$O), [(AuPEt$_3$)$_2$-o-hpspa] (**5**), [(AuPEt$_3$)$_2$-p-hpspa]·3H$_2$O (**6**·3H$_2$O), and [(AuPEt$_3$)$_2$tspa]·3H$_2$O (**9**·3H$_2$O) were solved by X-ray diffraction. **1**·3H$_2$O, **6**·3H$_2$O, and **9**·3H$_2$O were shown to contain tetranuclear Au$_4$ units separated by clusters of six water molecules, a situation that gave us the opportunity to analyze the influence of the environment on the structural parameters of the cluster. These clusters are absent in the structure of **5**, which only contains dinuclear units.

The antiinflammatory activity of the complexes was tested, and the o-h-pspa, tspa, and fspa derivatives proved to be the most active.

(5) Kerimova, A. A.; Atalay, M.; Ysifov, E. Y.; Kuprin, S. P.; Kerimov, T. M. *Pathophysiology* **2000**, *7*, 209.
(6) Hashimoto, K.; Whitehurst, C. E.; Matsubara, T.; Hirohata, K.; Lipsky, P. E. *J. Clin. Invest.* **1992**, *89*, 1839.
(7) Rigobello, M. P.; Scutari, G.; Boscolo, R.; Bindoli, A. *Br. J. Pharmacol.* **2002**, *136*, 1162.
(8) Hall, T. J.; Jeker, H.; Nyugen, H.; Schaeublin, M. *Inflammation Res.* **1996**, *45*, 230.
(9) Jeon, K. I.; Byun, M. S.; Jue, D. M. *Exp. Mol. Med.* **2003**, *35*, 61.
(10) Hill, D. T.; Sutton, B. M. *Cryst. Struct. Commun.* **1980**, *9*, 679.
(11) Shaw, C. F. *Chem. Rev.* **1999**, *99*, 2589.
(12) Ahmad, S.; Isab, A. A.; Ali, S.; Al-Arfaj, A. R. *Polyhedron* **2006**, *25*, 1633.
(13) Mohamed, A. A.; Chen, J.; Bruce, A. E.; Bruce, M. R. M.; Krause Bauer, J. A.; Hill, D. T. *Inorg. Chem.* **2003**, *42*, 2203.
(14) Chen, J.; Jiang, T.; Wei, G.; Mohamed, A. A.; Homrighausen, C.; Krause Bauer, J. A.; Bruce, A. E.; Bruce, M. R. M. *J. Am. Chem. Soc.* **1999**, *121*, 9225.
(15) Mohamed, A. A.; Abdou, H. E.; Chen, J.; Bruce, A. E.; Bruce, M. R. M. *Comments Inorg. Chem.* **2002**, *23*, 321.
(16) Boles Bryan, D. L.; Mikuriya, Y.; Hempel, J. C.; Mellinger, D.; Hashim, M.; Pasternack, R. F. *Inorg. Chem.* **1987**, *26*, 4180.

Experimental Section

Materials and Methods. 2-Chlorobenzaldehyde, 2-methoxybenzaldehyde, 4-methoxybenzaldehyde, 2-hydroxybenzaldehyde, 4-hydroxybenzaldehyde, 3,5-dibromo-2-hydroxybenzaldehyde, 2-furancarboxaldehyde, 2-thiophenecarboxaldehyde, 2-pyridinecarboxaldehyde, cyclopentanone (all from Aldrich), benzaldehyde (Probus), rhodanine (Aldrich) and triethylphosphinegold(I) chloride (Aldrich) were used as supplied.

Elemental analyses were performed with a Fisons 1108 microanalyser. Mass spectra were recorded on a Kratos MS50TC spectrometer connected to a DS90 system and operating in FAB mode (*m*-nitrobenzyl alcohol, Xe, 8 eV; ca. 1.28×10^{-15} J); ions were identified by DS90 software, and the data characterizing peaks for the metalated species were calculated using the isotope ^{197}Au. IR spectra (KBr pellets or Nujol mulls) were recorded on a Bruker IFS66V FT-IR spectrophotometer and are reported in the synthesis section using the following abbreviations: vs = very strong, s = strong, m = medium, w = weak, sh = shoulder, br = broad. ^{1}H and ^{13}C NMR spectra in solution were recorded in dmso-d_6 or $CDCl_3$ at room temperature on a Bruker AMX 300 operating at 300.14 (^{1}H) and 75.40 MHz (^{13}C), using 5 mm o.d. tubes; chemical shifts, in ppm, are reported relative to TMS using the solvent signal (δ ^{1}H = 2.50 ppm; δ ^{13}C = 39.50 ppm for dmso-d_6 or δ ^{1}H = 7.26 ppm; δ ^{13}C = 77.00 ppm for $CDCl_3$) as reference, with the atoms numbered as in Scheme 2. ^{1}H−^{1}H COSY NMR spectra were recorded, and ^{1}H−^{13}C HMBC (Heteronuclear Multiple Bond Correlation) and HMQC (Heteronuclear Multiple Quantum Coherence) experiments were performed, using a Varian Inova 400 spectrometer. ^{31}P NMR spectra were recorded at 202.46 MHz on a Bruker AMX 500 spectrometer using 5 mm o.d. tubes and are reported in ppm relative to external H_3PO_4 (85%). Coupling constants are reported in Hz. All the physical measurements were carried out by the RIAIDT services of the University of Santiago de Compostela (USC).

Synthesis. The 3-(aryl)-2-sulfanylpropenoic acids were prepared by condensation of the appropriate aldehyde with rhodanine, subsequent hydrolysis in an alkaline medium, and acidification with aqueous HCl.[19,20] For the preparation of 2-cyclopentyliden-2-sulfanylacetic acid, (H_2cpa), a ketone (cyclopentanone) was used in the condensation reaction instead of an aldehyde.[21]

Complexes were prepared by adding $AuPEt_3Cl$ in a 2:1 molar ratio to a solution of the appropriate sulfanylcarboxylic acid and NaOH in methanol/water. After stirring for 1 h, the methanol was evaporated in air or under vacuum. In cases where a solid was formed it was washed with water and dried in vacuo. In cases where an oil was obtained (**4**, **8**, **10**, **11**) it was treated with chloroform, filtered to remove NaCl, and the solvent was removed and the oil dried under vacuum.

[(AuPEt$_3$)$_2$pspa] (1). H_2pspa (0.038 g, 0.21 mmol), $AuPEt_3Cl$ (0.150 g, 0.43 mmol), methanol (8 cm^3), NaOH (0.017 g, 0.43 mmol), H_2O (1 cm^3), yellow solid. Yield: 86%. (Found: C 30.9, H 4.8, S 3.9%. Calcd for $C_{21}H_{36}O_2SP_2Au_2$: C 31.2, H 4.5, S 4.0%). MS (FAB): the main metalated signals are at *m*/*z* 1123 (13%), $[(AuPEt_3)_3pspa]^+$; 977 (100), $[(AuPEt_3)_3S]^+$; 859 (14) $[(AuPEt_3)_2AuS]^+$; 808 (39), $[M]^+$; 662 (4), $[(AuPEt_3)_2S]^+$; 433 (71), $[Au(PEt_3)_2]^+$ and 315 (66), $[AuPEt_3]^+$. IR (cm^{-1}): 1573 vs, ν_{as}(COO); 1336 s, ν_{sym}(COO); 1454 s, 1415 m, 1381 m, ν(PEt_3). NMR (dmso-d_6): ^{1}H, δ 7.43 (s, 1H, C(3)H), 8.05 (d, 2H, C(5)H, C(9)H), 7.36 (t, 2H, C(6)H, C(8)H), 7.25 (m, 1H, C(7)H), 1.92 (m, 12H, H(PCH_2)), 1.09 (m, 18H, H(PCH_3)); ^{13}C, δ 170.9 C(1), 127.4 C(2), 136.8 C(3), 134.4 C(4), 133.6 C(5) and C(9), 127.7 C(6) and C(8), 130.2 C(7), 16.9 (d, J(C−P) = 37.0 (PCH_2)), 8.9 (PCH_3); ^{31}P {^{1}H}, δ 39.2 (s). NMR ($CDCl_3$): ^{1}H, δ 8.03 (s, 1H, C(3)H), 8.17 (d, 2H, C(5)H, C(9)H), 7.37 (m, 2H, C(6)H, C(8)H), 7.23 (m, 1H, C(7)H), 1.81 (m, 12, H(PCH_2)), 1.20 (m, 18H, H(PCH_3)); ^{13}C, δ - C(1), 127.8 C(2), 139.7 C(3), 136.6 C(4), 131.4 C(5), 127.7 C(6), 128.3 C(7), 18.0 (d, ^2J(^{13}C−^{31}P) = 35.4 (PCH_2)), 8.9 (s, PCH_3); ^{31}P {^{1}H}, δ 38.7 (s). Single crystals of [($AuPEt_3$)$_2$pspa]·3H_2O (**1**·3H_2O) were grown by slow evaporation of the mother liquor.

[(AuPEt$_3$)$_2$Clpspa] (2). H_2Clpspa (0.046 g, 0.21 mmol), $AuPEt_3Cl$ (0.150 g, 0.43 mmol), methanol (8 cm^3), NaOH (0.017 g, 0.43 mmol), H_2O (1 cm^3), pale yellow solid. Yield: 82%. (Found: C 29.6, H 4.0, S 3.7%. Calcd for $C_{21}H_{35}O_2SClP_2Au_2$: C 29.9, H 4.2, S 3.8%). MS (FAB): the main metalated signals are at *m*/*z* 1157 (15%), $[(AuPEt_3)_3Clpspa]^+$; 977 (67), 859 (15) $[(AuPEt_3)_2AuS]^+$; $[(AuPEt_3)_3S]^+$; 842 (25), $[M]^+$; 662 (7), $[(AuPEt_3)_2S]^+$; 433 (100), $[Au(PEt_3)_2]^+$ and 315 (87), $[Au(PEt_3)]^+$. IR (cm^{-1}): 1580 vs, ν_{as}(COO); 1346 s, ν_{sym}(COO); 1458 s, 1413 m, 1380 s, ν(PEt_3). NMR ($CDCl_3$): ^{1}H, δ 7.98 (s, 1H, C(3)H), 7.32 (d, 1H, C(6)H), 7.21 (st, 1H, C(7)H), 7.14 (m, 1H, C(8)H), 7.82 (d, 1H, C(9)H), 1.79 (m, 12H, H(PCH_2)), 1.13 (m, 18H, H(PCH_3)); ^{13}C, δ 170.2 C(1), 126.8 C(2), 134.4 C(3), 136.4 C(4), 134.1 C(5), 128.8 C(6), 128.4 C(7), 125.7 C(8), 132.1 C(9), 17.9 (d, ^2J(^{13}C−^{31}P) = 34.8 (PCH_2)), 9.0 (s, PCH_3); ^{31}P {^{1}H}, δ 39.7 (s).

[(AuPEt$_3$)$_2$-o-mpspa] (3). H_2-o-mpspa (0.045 g, 0.21 mmol), $AuPEt_3Cl$ (0.150 g, 0.43 mmol), methanol (8 cm^3), NaOH (0.017 g, 0.43 mmol), H_2O (1 cm^3), yellow solid. Yield: 84%. (Found: C 31.2, H 4.2, S 3.4%. Calcd for $C_{22}H_{38}O_3SP_2Au_2$: C 31.5, H 4.6, S 3.8%). MS (FAB): the main metalated signals are at *m*/*z* 1153 (15%), $[(AuPEt_3)_3$-o-mpspa$]^+$; 977 (84), 859 (13) $[(AuPEt_3)_2AuS]^+$; $[(AuPEt_3)_3S]^+$; 838 (52), $[M]^+$; 662 (22), $[(AuPEt_3)_2S]^+$; 433 (89), $[Au(PEt_3)_2]^+$ and 315 (100), $[AuPEt_3]^+$. IR (cm^{-1}): 1570 sh, ν_{as}(COO); 1358 s, ν_{sym}(COO); 2834 w, ν_{sym}(OCH_3); 1457 vs, 1412 m, 1382 s, ν(PEt_3). NMR (dmso-d_6): ^{1}H, δ 7.59 (s, 1H, C(3)H), 8.31 (d, 1H, C(6)H), 6.89 (st, 1H, C(7)H), 7.13 (st, 1H, C(8)H), 6.79 (d, 1H, C(9)H), 3.75 (s, 3H, OCH_3), 1.85 (m, 12H, H(PCH_2)), 1.08 (m, 18H, H(PCH_3)); ^{13}C, δ - C(1), 119.1 C(2), - C(3), 125.0 C(4), 157.5 C(5), 110.0 C(6), 129.9 C(7), 127.0 C(8), 127.2 C(9), 55.0 C(OCH_3), 17.1 (d, ^2J(^{13}C−^{31}P) = 34.9 (PCH_2)), 8.9 (s, PCH_3); ^{31}P {^{1}H}, δ 39 (s), 53.8 (s).

[(AuPEt$_3$)$_2$-p-mpspa] (4). H_2-p-mpspa (0.045 g, 0.21 mmol), $AuPEt_3Cl$ (0.150 g, 0.43 mmol), methanol (8 cm^3), NaOH (0.017 g, 0.43 mmol), H_2O (1 cm^3), yellow oil. Yield: 85%. (Found: C 31.7, H 4.4, S 3.5%. Calcd for $C_{22}H_{38}O_3SP_2Au_2$: C 31.5, H 4.6, S 3.8%). MS (FAB): the main metalated signals are at *m*/*z* 977 (45%), $[(AuPEt_3)_3S]^+$; 859 (12) $[(AuPEt_3)_2AuS]^+$; 838 (30), $[M]^+$; 524 (3) $[(AuPEt_3)$H-p-mpspa$]^+$; 433 (62), $[Au(PEt_3)_2]^+$ and 315 (100), $[AuPEt_3]^+$. IR (cm^{-1}): 1585 vs, ν_{as}(COO); 1319 s, ν_{sym}(COO); 2834 m, ν_{sym}(OCH_3); 1455 vs, 1415 vs, 1380 m, ν(PEt_3). NMR (dmso-d_6): ^{1}H, δ 7.65 (s, 1H, C(3)H), 7.76 (d, 2H,C(5)H, C(9)H), 6.95 (d, 2H, C(6)H, C(8)H), 3.77 (s, 3H, OCH_3), 1.83 (m, 12H, H(PCH_2)), 1.07 (m, 18H, H(PCH_3)); ^{13}C, δ 168.5 C(1), 129.4 C(2), 135.6 C(3), 130.9 C(4), 131.6 C(5) and C(9), 113.2 C(6) and C(8), 158.5 C(7), 55.0 C(OCH_3), 17.3 (d, ^2J(^{13}C−^{31}P) = 34.9 (PCH_2)), 8.9 (s, PCH_3); ^{31}P {^{1}H}, δ 38.6 (s).

[(AuPEt$_3$)$_2$-o-hpspa] (5). H_2-o-hpspa (0.042 g, 0.21 mmol), $AuPEt_3Cl$ (0.150 g, 0.43 mmol), methanol (8 cm^3), NaOH (0.017 g, 0.43 mmol), H_2O (1 cm^3), orange solid. Yield: 91%. (Found: C 30.1, H 4.0, S 3.6%. Calcd for $C_{21}H_{36}O_3SP_2Au_2$: C 30.6, H 4.4, S

(17) Barreiro, E.; Casas, J. S.; Couce, M. D.; Sánchez, A.; Sordo, J.; Varela, J. M.; Vázquez-López, E. M. *Dalton Trans.* **2003**, 4754.
(18) Allen, F. H. *Acta Crystallogr.* **2002**, *B58*, 380.
(19) Gränacher, C. *Helv. Chim. Acta* **1922**, *5*, 610.
(20) Campaigne, E.; Cline, R. E. *J. Org. Chem.* **1956**, *21*, 32.
(21) Brown, F. C.; Bradsher, K.; McCallum, S. G.; Potter, M. *J. Org. Chem.* **1950**, *15*, 174.

3.9%). MS (FAB): the main metalated signals are at *m*/*z* 1139 (7%), $[(AuPEt_3)_3\text{-o-hpspa}]^+$; 977 (100), $[(AuPEt_3)_3S]^+$; 859 (13) $[(AuPEt_3)_2AuS]^+$; 824 (13), $[M]^+$; 662 (17), $[(AuPEt_3)_2S]^+$; 433 (47), $[Au(PEt_3)_2]^+$ and 315 (45), $[AuPEt_3]^+$. IR (cm^{-1}): 1568 s, ν_{as}(COO); 1335 m, ν_{sym}(COO); 1450 vs, 1413 s, 1381 s, ν(PEt_3). NMR (dmso-d_6): ^1H, δ 7.57 (s, 1H, C(3)H), 8.08 (s, 1H, C(5)OH), 6.80 (d, 1H, C(6)H), 6.95 (st, 1H, C(7)H), 6.72 (st, 1H, C(8)H), 8.15 (d, 1H, C(9)H), 1.87 (m, 12H, H(PCH_2)), 1.09 (m, 18H, H(PCH_3)); ^{13}C, δ 169.6 C(1), 120.8 C(2), 125.1 C(3), 127.0 C(4), 155.8 C(5), 116.3 C(6), 129.8 C(7), 118.7 C(8), 126.6 C(9), 18.0 (d, $^2J(^{13}C-^{31}P)$ = 34.9 (PCH_2)), 8.9 (s, PCH_3); ^{31}P {^1H}, δ 39.1 (s), 5.8 (s). Single crystals were grown by slow evaporation of a dmso-d_6 solution.

$[(AuPEt_3)_2$-p-hpspa] (6). H_2-p-hpspa (0.042 g, 0.21 mmol), $AuPEt_3Cl$ (0.150 g, 0.43 mmol), methanol (8 cm^3), NaOH (0.017 g, 0.43 mmol), H_2O (1 cm^3), yellow solid. Yield: 76%. (Found: C 30.1, H 4.6, S 3.6%. Calcd for $C_{21}H_{36}O_3SP_2Au_2$: C 30.6, H 3.4, S 3.9%). MS (FAB): the main metalated signals are at *m*/*z* 1139 (11%), $[(AuPEt_3)_3$-p-hpspa$]^+$; 977 (65), $[(AuPEt_3)_3S]^+$; 859 (9) $[(AuPEt_3)_2AuS]^+$; 824 (45), $[M]^+$; 662 (9), $[(AuPEt_3)_2S]^+$; 433 (100), $[Au(PEt_3)_2]^+$ and 315 (93), $[AuPEt_3]^+$. IR (cm^{-1}): 1565 vs, ν_{as}(COO); 1334 s, ν_{sym}(COO); 1453 vs, 1416 m, 1382 m, ν(PEt_3). NMR (dmso-d_6): ^1H, δ 7.28 (s, 1H, C(3)H), 7.76 (d, 2H, C(5)H, C(9)H), 6.67 (d, 2H, C(6)H, C(8)H), 9.46 (s, 1H, C(7)OH), 1.90 (m, 12H, H(PCH_2)), 1.09 (m, 18H, H(PCH_3)); ^{13}C, δ 172.8 C(1), 128.3 C(2), 129.9 C(3), 132.4 C(4), 130.7 C(5) and C(9), 114.2 C(6) and C(8), 155.2 C(7), 17.3 (d, J(C−P) = 33.7 (PCH_2)), 9.1 (PCH_3); ^{31}P {^1H}, δ 39.1 (s), 54.2 (s). NMR ($CDCl_3$) ^1H, δ 7.96 (s, 1H, C(3)H), 7.63 (d, 2H, C(5)H, C(9)H), 6.99 (d, 2H, C(6)H, C(8)H), 9.71 (s, 1H, C(7)OH), 1.81 (m, 12H, H(PCH_2)), 1.26 (m, 18H, H(PCH_3)); ^{31}P {^1H}, δ 38.2 (s). Single crystals of $[(AuPEt_3)_2$-p-hpspa$]\cdot 3H_2O$ (**6**$\cdot 3H_2O$) were grown by slow evaporation of a methanol/acetone solution.

$[(AuPEt_3)_2$-diBr-o-hpspa] (7). H_2diBr-o-hspspa (0.045 g, 0.21 mmol), $AuPEt_3Cl$ (0.150 g, 0.43 mmol), methanol (8 cm^3), NaOH (0.017 g, 0.43 mmol), H_2O (1 cm^3), orange solid. Yield: 85%. (Found: C 25.9, H 3.6, S 3.4%. Calcd for $C_{21}H_{34}O_3SBr_2P_2Au_2$: C 25.7, H 23.5, S 3.2%). MS (FAB): the main metalated signals are at *m*/*z* 977 (100%), $[(AuPEt_3)_3S]^+$; 982 (2), $[M]^+$; 662 (13), $[(AuPEt_3)_2S]^+$; 433 (18), $[Au(PEt_3)_2]^+$ and 315 (18), $[AuPEt_3]^+$. IR (cm^{-1}): 1577 vs, ν_{as}(COO); 1316 m, ν_{sym}(COO); 1439 m, 1401 s, 1383 vs, ν(PEt_3). NMR ($CDCl_3$): ^1H, δ 7.79 (s, 1H, C(3)H), 9.91 (s, 1H, C(5)OH), 7.62 (s, 1H, C(7)H), 7.32 (s, 1H, C(9)H), 1.83 (m, 12H, H(PCH_2)), 1.17 (m, 18H, H(PCH_3)); ^{13}C, δ 169.6 C(1), 124.7 C(2), 133.8 C(3), 126.8 C(4), 150.0 C(5), 110.0 C(6), 139.5 C(7), 111.7 C(8), 136.5 C(9), 18.7 (d, $^2J(^{13}C-^{31}P)$ = 33.4 (PCH_2)), 9.7 (s, PCH_3); ^{31}P {^1H}, δ 37.8 (s), 56.1 (s).

$[(AuPEt_3)_2$fspa] (8). H_2fspa (0.037 g, 0.21 mmol), $AuPEt_3Cl$ (0.150 g, 0.43 mmol), methanol (8 cm^3), NaOH (0.017 g, 0.43 mmol), H_2O (1 cm^3), brown oil. Yield: 86%. (Found: C 28.3, H 4.7, S 3.9%. Calcd for $C_{19}H_{34}O_3SP_2Au_2$: C 28.6, H 4.3, S 4.0%). MS (FAB): the main metalated signals are at *m*/*z* 1113 (24%), $[(AuPEt_3)_3$fspa$]^+$; 977 (66), $[(AuPEt_3)_3S]^+$; 859 (11) $[(AuPEt_3)_2AuS]^+$; 798 (46), $[M]^+$; 662 (6), $[(AuPEt_3)_2S]^+$; 482 (3), $[(AuPEt_3)Hfspa]^+$; 433 (100), $[Au(PEt_3)_2]^+$ and 315 (76), $[AuPEt_3]^+$. IR (cm^{-1}): 1580 vs, ν_{as}(COO); 1335 m, ν_{sym}(COO); 1456 m, 1416 m, 1379 m, ν(PEt_3). NMR (dmso-d_6): ^1H, δ 7.59 (s, 1H, C(3)H), 7.18 (d, 1H, C(5)H), 6.61 (t, 1H, C(6)H), 7.69 (d, 1H, C(7)H), 1.85 (m, 12H, H(PCH_2)), 1.07 (m, 18H, H(PCH_3)); ^{13}C, δ 168.0 C(1), 126.0 C(2), 129.9 C(3), 152.0 C(4), 113.4 C(5), 112.1 C(6), 143.4 C(7), 17.7 (d, J(C−P) = 34.5 (PCH_2)), 9.4 (PCH_3). NMR ($CDCl_3$): ^1H, δ 8.0 (s, 1H, C(3)H), 7.11 (d, 1H, C(5)H), 6.45 (t, 1H, C(6)H), 7.40 (d, 1H, C(7)H), 1.83 (m, 12H, H(PCH_2)), 1.19 (m, 18H, H(PCH_3)); ^{13}C, δ 169.0 C(1), 116.1 C(2), 128.4 C(3), 152.9 C(4), 112.3 C(5), 111.7 C(6), 142.9 C(7), 18.0 (d, $^2J(^{13}C-^{31}P)$ = 35.3 (PCH_2)), 8.9 (s, PCH_3);^{31}P {^1H}, δ 38.8(s), 54.7 (s).

$[(AuPEt_3)_2$tspa] (9). H_2tspa (0.041 g, 0.21 mmol), $AuPEt_3Cl$ (0.150 g, 0.43 mmol), methanol (8 cm^3), NaOH (0.017 g, 0.43 mmol), H_2O (1 cm^3), pale yellow solid. Yield: 74%. (Found: C 27.9, H 4.6, S 7.6%. Calcd for $C_{19}H_{34}O_2S_2P_2Au_2$: C 28.0, H 4.2, S 7.9%). MS (FAB): the main metalated signals are at *m*/*z* 1129 (20%), $[(AuPEt_3)_3$fspa$]^+$; 977 (80), $[(AuPEt_3)_3S]^+$; 859 (11) $[(AuPEt_3)_2AuS]^+$; 814 (54), $[M]^+$; 662 (8), $[(AuPEt_3)_2S]^+$; 433 (100), $[Au(PEt_3)_2]^+$ and 315 (82), $[AuPEt_3]^+$. IR (cm^{-1}): 1571 vs, ν_{as}(COO); 1331 s, ν_{sym}(COO); 1455 s, 1416 m, 1379 m, ν(PEt_3). NMR (dmso-d_6): ^1H, δ 7.86 (s, 1H, C(3)H), 7.31 (d, 1H, C(5)H), 7.08 (t, 1H, C(6)H), 7.50 (d, 1H, C(7)H), 1.89 (m, 12H, H(PCH_2)), 1.11 (m, 18H, H(PCH_3)); ^{13}C, δ 169.7 C(1), 126.4 C(2), 128.9 C(3), 141.5 C(4), 128.0 C(5), 125.9 C(6), 127.1 C(7), 17.2 (d, J(C−P) = 35.1 (PCH_2)), 9.00 (PCH_3). NMR ($CDCl_3$): ^1H, δ 8.16 (s, 1H, C(3)H), 7.25 (d, 1H, C(5)H), 6.96 (t, 1H, C(6)H), 7.27 (d, 1H, C(7)H), 1.76 (m, 12H, H(PCH_2)), 1.01 (m, 18H, H(PCH_3)); ^{13}C, δ 171.3 C(1), 128.9 C(2), 132.2 C(3), 141.3 C(4), 132.2 C(5), 126.0 C(6), 127.0 C(7), 18.0 (d, $^2J(^{13}C-^{31}P)$ = 35.3 (PCH_2)), 8.9 (s, PCH_3); ^{31}P {^1H}, δ 39.1 (s), 54.7(s). Single crystals of $[(AuPPh_3)_2$-tspa$]\cdot 3H_2O$ (**9**$\cdot 3H_2O$) were grown by slow evaporation of the mother liquor.

$[(AuPEt_3)_2$-o-pyspa] (10). H_2-o-pypspa (0.039 g, 0.21 mmol), $AuPEt_3Cl$ (0.150 g, 0.43 mmol), methanol (8 cm^3), NaOH (0.017 g, 0.43 mmol), H_2O (1 cm^3), orange oil. Yield: 74%. (Found: C 30.0, H 4.7, N 1.9, S 3.6%. Calcd for $C_{20}H_{35}O_2SNP_2Au_2$: C 29.7, H 4.4, N 1.7, S 3.9%). MS (FAB): the main metalated signals are at *m*/*z* 1124 (2%), $[(AuPEt_3)_3$-o-pyspa$]^+$; 977 (23), $[(AuPEt_3)_3S]^+$; 859 (3) $[(AuPEt_3)_2AuS]^+$; 809 (10), $[M]^+$; 662 (6), $[(AuPEt_3)_2S]^+$; 495 (4), $[(AuPEt_3)$H-o-pyspa$]^+$; 433 (100), $[Au(PEt_3)_2]^+$ and 315 (44), $[AuPEt_3]^+$. IR (cm^{-1}): 1556 vs, ν_{as}(COO); 1341 s, ν_{sym}(COO); 1454 vs, 1431 s, 1380 s, ν(PEt_3). NMR (dmso-d_6): ^1H, δ 7.47 (s, 1H, C(3)H), 8.55 (d, 1H,C (5)H), 7.78 (st, 1H, C(6)H), 7.20 (st, 1H, C(7)H), 8.63 (d, 1H, C(8)H), 1.90 (m, 12H, H(PCH_2)), 1.08 (m, 18H, H(PCH_3)); ^{13}C, δ 170.6 C(1), 138.9 C(2), 135.5 C(3), 155.6 C(4), 149.0 C(5), 133.8 C(6), 121.6 C(7), 124.5 C(8), 17.0 (d, $^2J(^{13}C-^{31}P)$ = 36.3 (PCH_2)), 8.9 (s, PCH_3); ^{31}P {^1H}, δ 38.1 (s).

$[(AuPEt_3)_2$cpa] (11). H_2cpa (0.034 g, 0.21 mmol), $AuPEt_3Cl$ (0.150 g, 0.43 mmol), methanol (8 cm^3), NaOH (0.017 g, 0.43 mmol), H_2O (1 cm^3), brown oil. Yield: 73%. (Found: C 28.5, H 4.9, N 4.7, S 4.3%. Calcd for $C_{19}H_{38}O_2SP_2Au_2$: C, 29.0; H, 5.0; S, 4.0%). MS (FAB): the main metalated signals are at *m*/*z* 1101 (7%), $[(AuPEt_3)_3$cpa$]^+$; 977 (100), $[(AuPEt_3)_3S]^+$; 859 (13) $[(AuPEt_3)_2AuS]^+$; 786 (68), $[M]^+$; 662 (7), $[(AuPEt_3)_2S]^+$; 471 (3), $[(AuPEt_3)$Hcpa$]^+$; 433 (38), $[Au(PEt_3)_2]^+$ and 315 (56), $[AuPEt_3]^+$. IR (cm^{-1}): 1554 vs, ν_{as}(COO); 1365 sh, ν_{sym}(COO); 1452 vs, 1411 vs, 1380 vs, ν(PEt_3). NMR (dmso-d_6): ^1H, δ 2.68 (m, 2H, C(4)H_2), 1.58 (m, 2H, C(5)H_2), 1.58 (m, 2H, C(6)H_2), 2.58 (m, 2H, C(7)H_2), 1.89 (m, 12H, H(PCH_2)), 1.08 (m, 18H, H(PCH_3));^{13}C δ 169.8 C(1), 122.1 C(2), 151.6 C(3), 36.1 C(4), 27.2 C(5), 25.5 C(6), 34.4 C(7), 17.2 (d, $^2J(^{13}C-^{31}P)$ = 34.1 (PCH_2)), 8.9 (s, PCH_3); ^{31}P {^1H}, δ 38.6 (s).

X-ray Structure Determination. Single crystals of $[(AuPEt_3)_2$-pspa$]\cdot 3H_2O$ (**1**$\cdot 3H_2O$), $[(AuPEt_3)_2$-o-hpspa] (**5**), $[(AuPEt_3)_2$-p-hpspa$]\cdot 3H_2O$ (**6**$\cdot 3H_2O$), and $[(AuPEt_3)_2$tspa$]\cdot 3H_2O$ (**9**$\cdot 3H_2O$) were mounted on glass fibers for data collection in a Bruker Smart CCD automatic diffractometer at 293 K using Mo Kα radiation (λ = 0.71073 Å). The crystal data, experimental details, and refinement results are summarized in Table 1. Corrections for Lorentz effects,

Table 1. Crystal Data For [$(AuPEt_3)_2$pspa]·$3H_2O$ (**1**·$3H_2O$), [$(AuPEt_3)_2$-o-hpspa] (**5**), [$(AuPEt_3)_2$-p-hpspa]·$3H_2O$ (**6**·$3H_2O$), and [$(AuPEt_3)_2$tspa]·$3H_2O$ (**9**·$3H_2O$)

compound	[$(AuPEt_3)_2$pspa]·$3H_2O$ (**1**·$3H_2O$)	[$(AuPEt_3)_2$-o-hpspa] (**5**)	[$(AuPEt_3)_2$-p-hpspa]·$3H_2O$ (**6**·$3H_2O$)	[$(AuPEt_3)_2$tspa]·$3H_2O$·(**9**·$3H_2O$)
empirical formula	$C_{21}H_{42}Au_2O_5P_2S_2$	$C_{21}H_{36}O_3SAu_2P_2$	$C_{21}H_{42}Au_2O_6P_2S$	$C_{19}H_{40}Au_2O_5P_2S_2$
M	862.48	824.43	878.42	868.50
crystal system	monoclinic	monoclinic	triclinic	monoclinic
space group	*C*2/*m*	*P*2(1)/*n*	$P\bar{1}$	*C*2/*m*
a (Å)	15.0355(16)	11.1140(9)	10.818(2)	14.9284(11)
b (Å)	15.9279(16)	15.3963(13	11.155(2)	15.9503(12)
c (Å)	13.5192(14)	16.2397(13)	13.509(3)	13.3470(13)
α (°)	90	90	111.044(4)	90
β (°)	117.178(2)	108.265(2)	105.415(3)	116.077(2)
γ (°)	90	90	92.047(4)	90
V (Å^3)	2880.2(5)	2638.8(4)	1451.0(5)	2854.6(4)
Z	4	4	2	4
D_c (Mg. M^{-3})	1.989	2.075	2.011	2.021
M (mm^{-1})	10.386	11.325	10.312	10.550
crystal size (mm^3)	0.28 × 0.22 × 0.22	0.39 × 0.20 × 0.17	0.40 × 0.20 × 0.20	0.25 × 0.12 × 0.10
θ range for data collection (°)	1.69−28.00	1.87−28.00	1.97−27.98	1.70−28.03
index ranges	$-14 \le h \le 19$ $-20 \le k \le 20$, $-17 \le l \le 17$	$-14 \le h \le 14$ $-16 \le k \le 20$, $-21 \le l \le 14$	$-13 \le h \le 14$, $-14 \le k \le 10$, $-17 \le l \le 16$	$-19 \le h \le 13$ $-18 \le k \le 21$ $-15 \le l \le 17$
reflections collected	7741	16979	8039	7720
unique reflections, *R*	3259 [*R*(int) = 0.0932]	6283 [*R*(int) = 0.1033]	5647 [*R*(int) = 0.0447]	3235 [*R*(int) = 0.0849]
Final R1, wR2 [$I > 2\sigma(I)$]	0.0520, 0.1034	0.0446, 0.0783	0.0620, 0.1159	0.0485, 0.0948
(All data)	0.1978, 0.1308	0.1004, 0.0895	0.1370, 0.1530	0.1974, 0.1197

polarization,[22] and absorption[23] were made. In **1**·$3H_2O$ the hydrogen atoms of the water molecules were not located so the hydrogen bonds were determined on the basis of the O···O distances. In **5** the ethyl groups of the triethylphosphine fragments are disordered, the hydrogen of O(3) was refined. In **6**·$3H_2O$ the hydrogen atoms of the water molecules were not located, so the hydrogen bonds were determined on the basis of the O···O distances. In **9**·$3H_2O$ the thiophene group is disordered (two positions). Once again, the hydrogen atoms of the water molecules were not located.

In Vivo Anti-inflammatory Experiments. Animals. Sprague−Dawley rats weighting 175−200 g were used. For 1 week before the experiment the animals were maintained in a sound-proofed room thermostatted at 22 ± 1 °C with an artificial 12 h:12 h light: dark cycle. Food and sterile water were supplied ad libitum.

Paw Edema Test (Anti-inflammatory Activity). Solutions of the compounds under investigation in water/polyethylene glycol (3:2), or vehicle alone, were administered intraperitoneally 30 min before edema was induced by injection of 0.05 mL of a 1% suspension of carrageenan in 0.9% sterile saline into the right plantar aponerurosis of the rat.[24] Paw volume was measured with a Ugo Basile 7140 plethysmometer before and 4 h after the injection of carrageenan. Anti-inflammatory activity is expressed as percentage reduction of edema in treated rats in comparison with controls; values are the mean ± SE of 8−12 rats. To assess statistical contrast the Student-*t* test was carried out, and values were considered statistically significant when $P < 0.05$.

Results and Discussion

The complexes were prepared by adding a solution of $Au(PEt_3)Cl$ in a 2:1 molar ratio to a solution of the appropriate acid and NaOH in methanol. The FAB^+ mass spectra of these complexes show the $[M]^+$ peak and other fragments that, as in similar systems,[25–27] are indicative of cleavage of the Au−S and Au−P bonds. The complexes are soluble in MeOH, EtOH, acetone, DMSO, and $CHCl_3$ but are insoluble in water and Et_2O.

Description of the Structures. [$(AuPEt_3)_2$pspa]·$3H_2O$ (1·$3H_2O$), [$(AuPEt_3)_2$-p-hpspa]·$3H_2O$ (6·$3H_2O$) and [$(AuPEt_3)_2$tspa]·$3H_2O$ (9·$3H_2O$). Crystals of **1**·$3H_2O$ and **9**·$3H_2O$ are both monoclinic, space group *C*2/*m*, whereas those of **6**·$3H_2O$ are triclinic, space group $P\bar{1}$. The most significant structural parameters for these compounds are shown in Tables 2 and 3.

The three crystals contain $[(AuPEt_3)_2L]_2$ dimeric units and water molecules. The dimer units can be seen as consisting of two monomer units that dimerize through Au(I)−Au(I) interactions. In the monomeric unit [$(AuPEt_3)_2$pspa] (Figure 1) the two gold atoms have equivalent coordinative environments. Each one is bonded to the S atom of the sulfanyl group and to the P atom of PEt_3; the orientation of the carboxylate group allows both Au atoms to interact with O(1) [Au−O(1) 2.992(14) Å, less than the sum of the van der Waals radii, 3.20 Å].[28]

The Au···Au distances within the unit [Au−Au#1 3.1997(11) Å] are less than the sum of the van der Waals radii (3.70 Å)[28] but each unit is also close to a neighboring molecule with Au−Au#2 distances of 3.2376(12) Å, which are again less than the sum of the van der Waals radii. Thus, the structure can be seen as a dimer of the type Au_4S_2, as shown in Figure 2, where the ethyl groups of the phosphine have been omitted for clarity.

(22) *SAINT:SAX Area Detector Integration*; Bruker AXS, Inc.: Madison, WI, 1996.
(23) Sheldrick G. M. *SADABS*, Version 2.03; University of Göttingen, Göttingen, Germany, 2002.
(24) Winter, C. A.; Risley, E. A.; Nuss, G. W. *Proc. Soc. Ext. Biol. Med.* **1962**, *111*, 544.
(25) Cookson, P. D.; Tiekink, E. R. T. *J. Coord. Chem.* **1992**, *26*, 313.
(26) Cookson, P. D.; Tiekink, E. R. T. *J. Crystallogr. Spectrosc. Res.* **1993**, *23*, 231.
(27) Wilton-Ely, J. D. E. T.; Schier, A.; Mitzel, N. W.; Schmidbaur, H. *J. Chem. Soc., Dalton Trans.* **2001**, 1058.
(28) Huheey, J. E.; Keiter, E. A.; Keiter, R. L. *Inorganic Chemistry. Principles of Structure and Reactivity*, 4th ed.; Harper Collins: New York, 1993.

Table 2. Selected Bond Lengths (Å) and Angles (°) in $[(AuPEt_3)_2pspa]\cdot 3H_2O$ (**1**·$3H_2O$) and $[(AuPEt_3)_2tspa]\cdot 3H_2O$ (**9**·$3H_2O$)[a]

	1·$3H_2O$	**9**·$3H_2O$
(a) Au Environment		
Au−P	2.256(4)	2.261(4)
Au−S	2.349(4)	2.350(4)
Au−O(1)	2.992(14)	2.985(13)
Au−Au#1	3.1997(11)	3.2423(10)
Au−Au#2	3.2376(12)	3.3121(10)
P−Au−S	175.40(16)	175.06(15)
P−Au−O(1)	111.6(3)	110.8(3)
S−Au−O(1)	65.0(3)	66.1(3)
P−Au−Au#1	134.38(13)	135.78(11)
S−Au−Au#1	47.07(9)	46.39(8)
O(1)−Au-Au#1	57.68(16)	57.10(16)
P−Au−Au#2	107.35(12)	108.32(10)
S−Au−Au#2	76.47(11)	75.29(11)
O(1)−Au-Au#2	140.5(3)	140.4(2)
Au#1−Au-Au#2	90.0	90.000(1)
C(2)−S-Au	103.5(5)	104.8(6)
C(2)−S-Au#1	103.5(5)	104.8(6)
Au−S−Au#1	85.86(18)	87.23(17)
C(1)−O(1)−Au	105.4(14)	102.0(15)
O(1W)-O(1)-Au	107.9(7)	112.3(7)
(b) Ligand		
S−C(2)	1.74(2)	1.73(2)
O(1)−C(1)	1.12(2)	1.16(2)
O(2)−C(1)	1.23(2)	1.27(2)
C(1)−C(2)	1.46(3)	1.53(3)
C(2)−C(3)	1.41(2)	1.36(2)
C(3)−C(4)	1.43(2)	1.48(3)
O(2)−C(1)−O(1)	122(2)	123(3)
O(2)−C(1)−C(2)	120(2)	115(2)
O(1)−C(1)−C(2)	118(2)	122(2)
C(3)−C(2)−C(1)	117.5(18)	117(2)
C(3)−C(2)−S	121.4(15)	126.7(17)
C(1)−C(2)−S	121.1(15)	116.1(17)
C(2)−C(3)−C(4)	133.5(19)	127(2)

[a] Symmetry transformations used to generate equivalent atoms: #1, x, $-y+1$, z; #2, $-x$, y, $-z$.

Table 3. Selected Bond Lengths (Å) and Angles (°) in $[(AuPEt_3)_2$-p-hpspa$]\cdot 3H_2O$ (**6**·$3H_2O$)[a]

(a) Au Environment			
Au(1)−P(1)	2.268(4)	P(1)−Au(1)−S	174.57(14)
Au(1)−S	2.350(3)	P(1)−Au(1)−Au(2)	133.84(13)
Au(1)−Au(2)	3.2000(9)	C(2)−S−Au(1)	104.0(5)
Au(1)−O(1)	2.967(13)	P(1)−Au(1)−O(1)	108.3(3)
Au(2)−S	2.347(4)	S−Au(1)−O(1)	67.2(3)
Au(2)−P(2)	2.263(5)	P(1)−Au(1)−Au(2)#1	107.15(12)
Au(2)−O(1)	3.037(13)	S−Au(1)−Au(2)#1	77.83(8)
Au(2)−Au(1)#1	3.1864(9)	S−Au(1)−Au(2)	47.02(9)
		P(2)−Au(2)−S	175.48(14)
		P(2)−Au(2)−O(1)	110.2(3)
		S−Au(2)−O(1)	65.9(3)
		Au(1)−S−Au(2)	85.90(12)
		C(1)−O(1)−Au(2)	103.6(11)
		C(2)−S−Au(2)	105.0(5)
		Au(2)#1−Au(1)−Au(2)	89.86(2)
		S−Au(2)−Au(1)#1	78.02(8)
		P(2)−Au(2)−Au(1)#1	106.30(13)
(b) p-hpspa			
S−C(2)	1.783(12)	O(1)−C(1)−O(2)	123.0(16)
O(1)−C(1)	1.221(18)	O(1)−C(1)−C(2)	117.6(15)
O(2)−C(1)	1.249(17)	O(2)−C(1)−C(2)	119.2(16)
C(1)−C(2)	1.509(19)	C(3)−C(2)−C(1)	118.2(13)
C(2)−C(3)	1.360(18)	C(3)−C(2)−S	122.7(11)
C(3)−C(4)	1.42(2)	C(1)−C(2)−S	119.1(11)
		C(2)−C(3)−C(4)	133.8(13)

[a] Symmetry transformations used to generate equivalent atoms: #1, $-x+1$, $-y$, $-z$.

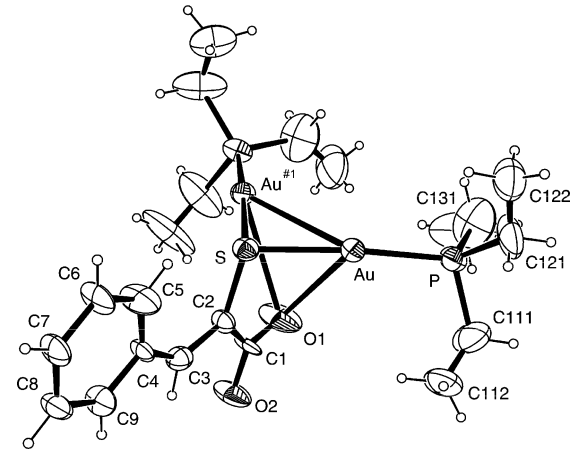

Figure 1. Crystal structure of the $[(AuPEt_3)_2pspa]$ unit. Ellipsoids are shown at the 30% probability level.

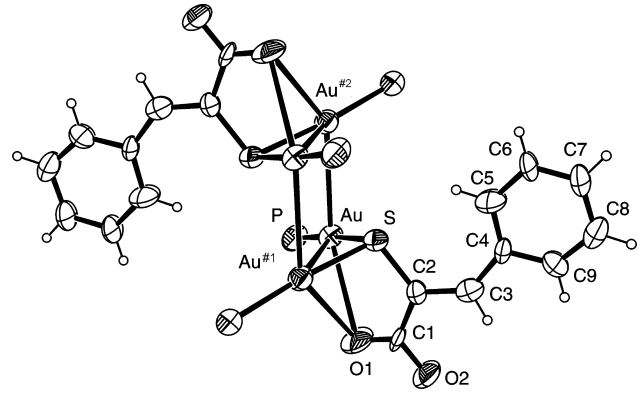

Figure 2. Structural representation of $[(AuPEt_3)_2pspa]_2$. Ellipsoids are shown at the 30% probability level. For the sake of clarity, the ethyl groups of PEt_3 are not shown.

This Au_4S_2 core is a fairly common structural motif for Au(I) sulfur clusters[29] but this is a very rare motif in situations like the ones described in this paper. Specifically, the Au···Au distances are slightly longer than those found in $[(AuPMe_3)_2(\mu\text{-tatg})]_2(NO_3)_2$,[13] [3.106(7), 3.171(11) Å], $[(AuPPh_3)_2(\mu\text{-}SC_6H_4CH_3)]_2(PF_6)_2$,[14] [3.152(1), 3.173(1) Å], $[(AuPPh_3)_2(\mu\text{-}SCH_2C_6H_5)]_2(BF_4)_2$,[30] [3.060(1), 3.078(1) Å], and also longer than the ones present in $[(AuPPh_3)_2$-$SCH_2COO(AuPPh_3)]_2(BF_4)_2$ and $[(AuPPh_3)_2S-C_6H_4-COOH]_2(BF_4)_2$[30] [3.1270(5) and 3.1628(4) Å], the only two sulfanylcarboxylates described in the literature that contain this cluster. The latter two compounds have the formation of the Au_4S_2 core in common with **1**·$3H_2O$, but there are also remarkable differences. For example, in the first case the existence of a third $AuPPh_3$ group coordinated to the carboxylate group [Au−O: 2.057(4) Å] moves this group away from the Au atoms bonded to the S atom. On the other hand, in the last compound the carboxylate group is protonated and only interacts with one of the Au atoms (Au−O: 2.778 Å); besides, this interacts through one F−H−O hydrogen bond with the tetrafluoroborate anion present in the structure.

(29) Gimeno, M. C.; Laguna, A. *Comprehensive Coordination Chemistry II*; Elsevier: Oxford, 2004; Vol. *6*, p 1058.
(30) Sladek, A.; Schneider, W.; Angermaier, K.; Bauer, A.; Schidbauer, H. *Z. Naturforsch.* **1996**, *516*, 765.

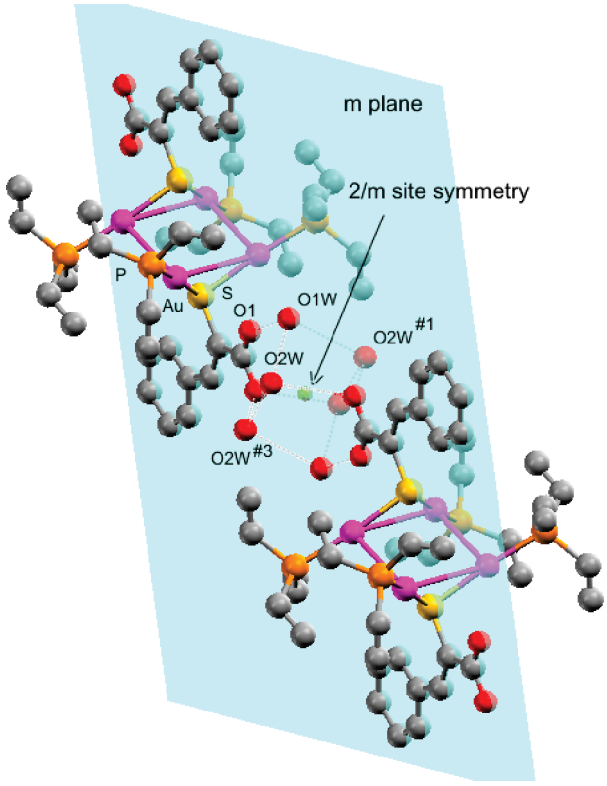

Figure 3. Position of the $(H_2O)_6$ cluster in the crystal of $[(AuPEt_3)_2pspa]\cdot 3H_2O$.

The water molecules present in the crystal interact with one another through hydrogen bonds to form an $(H_2O)_6$ cluster with a conformation of the "chair" type, which is similar to that found in the hexagonal compact structure of the Ih ice crystal. It was not possible to locate the hydrogen atoms of the water molecules and thus the hydrogen bonds must be described on the basis of the O···O distances, 2.784(18) Å for O(1W)−O(2W) and 2.80(2) Å for O(2W)−O(2W)#3; #3 = $-x + 1$, y, $-z + 1$. This cluster is located in the lattice in the *c* position in the Wyckoff terminology, with the $pspa^{2-}$ fragment of the dimer units located in the symmetry plane in which the two $AuPEt_3$ fragments are generated by a reflection (Figure 3). The repetition of $(H_2O)_6$ clusters and dimer units generates sheets.

Furthermore, at a distance of about 2.6 Å from the cluster there are two C(7)−H atoms of phenyl rings from one ligand of neighboring molecules from adjacent sheets. This gives rise to the environment for the cluster that is represented in Figure 4. The C−H···O parameters for these interactions [C(7)−H(7)···O(1W)#1: 0.93, 2.61, 3.40(3) Å, 143.3°; #1 x, y, $z - 1$] and for the [C(8)−H(8)···O(2)#2: 0.93, 2.58, 3.48(3) Å, 164.3°; #2 $-x + 1$, y, $-z$] suggest close contacts.[31]

The crystals of **6**·3H$_2$O and **9**·3H$_2$O consist of $[(AuPEt_3)_2xspa]_2$ units and $(H_2O)_6$ clusters, as in **1**·3H$_2$O.

The general coordinative scheme found in the $[(AuPEt_3)_2$-p-hpspa$]_2$ (Supporting Information, Figure S1) and $[(AuPEt_3)_2tspa]_2$ (Supporting Information, Figure S2) units is similar to that found in $[(AuPEt_3)_2pspa]_2$; however, some differences do warrant further comment.

The Au−Au distances [3.1997(11), 3.2376(12) for **1**·3H$_2$O; 3.2003(9), 3.1871(9) for **6**·3H$_2$O and 3.2423(10), 3.3121(10) Å for **9**·3H$_2$O] show that the greater metal−metal interaction is present in **6**·3H$_2$O, and it is also in this compound that the Au_4 ring is closest to a square. The Au−O bond distances [2.992(14) for **1**·3H$_2$O; 2.967(13), 3.037(13) for **6**·3H$_2$O and 2.985(13) Å for **9**·3H$_2$O] are all less than the sum of the van der Waals radii (3.20 Å)[28] but these show a weaker interaction than those previously found in the $[(AuPPh_3)_2xspa]$ complexes[17] and in **5** (vide infra).

The differences also affect the $(H_2O)_6$ cluster. It can be seen in Figure 5 that the environment of these clusters is different in the three crystals. Whereas in all cases the three O atoms of the cluster interact with O(1) and O(2) of the carboxylate group, thus generating the previously discussed sheets, the close contacts with other neighboring sheets are different. In **9**·3H$_2$O, besides the C(7)−H(7)−O(1W) interactions [C(7B)−H(7B)−O(1W)#2: 0.93, 2.59, 3.52(10) Å, 179.3°; #2, x, y, $z - 1$] that are also present in **1**·3H$_2$O, the O(2W)#1 atom interacts with the H-atom bonded to the triethylphosphine methyl group [C(121)−H(12B)−O(2W)#1: 0.97, 2.68, 3.60(2) Å, 157.6°; #1, $-x + 1/2$, $-y + 1/2$, $-z + 1$]. In **6**·3H$_2$O the interaction is with the H atom of the OH substituent on the phenyl ring of the p-mpspa ligand [O(3)−H···O(1W)#3 : 0.82, 1.79, 2.55(3) Å, 152.4°; #3, x, y, $z - 1$], thus leading to an environment with 6 O atoms for this cluster. These different environments and the structural packing have an influence on the cluster parameters, as shown in Table 4. The O···O bond distances range from 2.66(3) to 2.83(3) [2.75 Å for the Ih ice (T = 60 K), 2.85 Å for liquid water][32,33] and the angles [78.9(8) to 92.5(6)°] show the significant distortion of the cluster with respect to the ideal tetrahedral angle of Ih ice.

Two examples of $(H_2O)_6$ clusters that have a chair conformation and are located between metallic units have recently been described. One of these structures was identified in $[Cu(L)]_2[Mo(CN)_8]\cdot 3H_2O$ [L = 1,4-bis(3-aminopropylpiperazine)],[34] bonded through hydrogen bonds to the CN ligands of the $[Mo(CN)_8]^{4-}$ fragments that surround it. The other case is $Li_6[Ni_3V_{18}O_{42}(H_2O)_{12}(SO_4)]\cdot 24HO$,[35] which is bonded through one hydrogen bond to one terminal O atom of the $[V_{18}O_{42}(SO_4)]$ fragment.

In addition, genuine $(H_2O)_6$ clusters have been described that are bonded by hydrogen bonds to other water molecules, thus generating major entity structures. For example, in $\{[Mn(cda)_2\cdot H_2O]\cdot 4H_2O\}n$ (H_2cda = 4-hydroxypyridine-2,6-dicarboxylic acid)[36] the cluster is bonded to two acyclic tetramers to form an $(H_2O)_{14}$ entity, in 1,4-$[B(OH)_2]_2$-

(31) Desiraju, G. R.; Steiner, T. *The Weak Hydrogen Bond*; Oxford University Press: Oxford, U.K., 1999; p 29.
(32) Jeffrey, G. A. *An Introduction to Hydrogen Bonding*; Oxford University Press: New York, 1997.
(33) Kuhs, W. F.; Lehman, M. S. *J. Phys. Chem.* **1983**, *87*, 4312.
(34) Mukhopadhyay, U.; Bernal, I. *Cryst. Growth Des.* **2005**, *5*, 1687.
(35) Doedens, R. J.; Johannes, E.; Ishaque Khan, M. *Chem. Commun.* **2002**, 62.
(36) Ghosh, S. K.; Ribas, J.; El Fallah, M. S.; Bharadwaj, P. K. *Inorg. Chem.* **2005**, *44*, 3856.

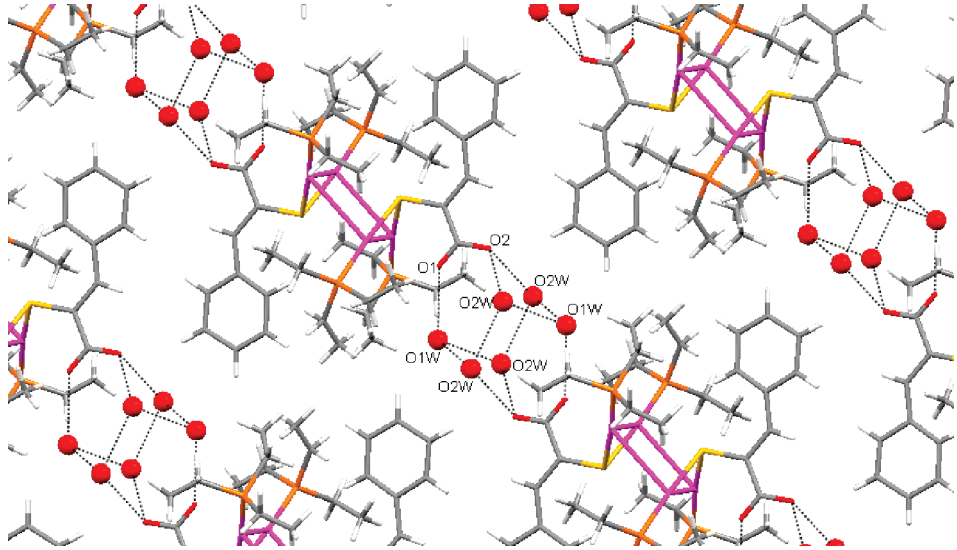

Figure 4. Close environment of the $(H_2O)_6$ cluster in $[(AuPEt_3)_2pspa]\cdot 3H_2O$.

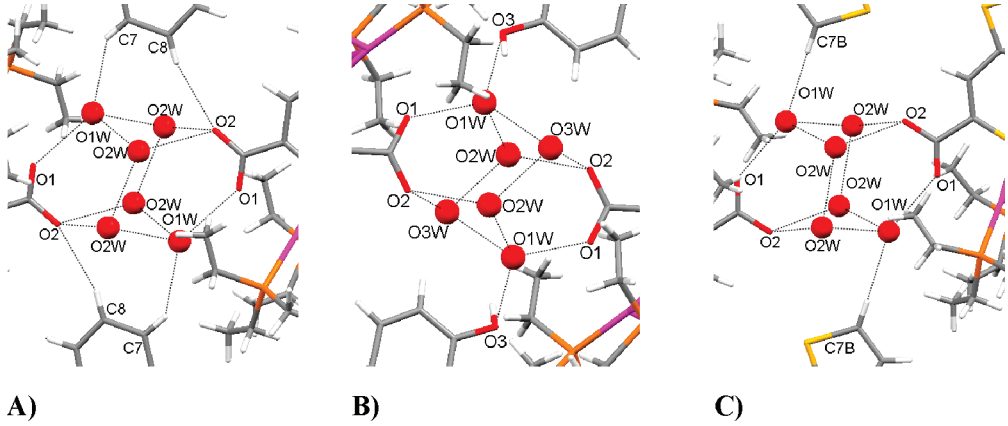

Figure 5. Environment of the $(H_2O)_6$ clusters in **1**·$3H_2O$ (**A**), **6**·$3H_2O$ (**B**), and **9**·$3H_2O$ (**C**).

Table 4. Structural Parameters of the $(H_2O)_6$ Clusters in the Crystals of **1**·$3H_2O$, **6**·$3H_2O$, and **9**·$3H_2O$[a]

interactions	**1**·$3H_2O$	**6**·$3H_2O$	**9**·$3H_2O$
O(1W)−O(2W)	2.784(18)	2.67(4)	2.720(19)
O(2W)−O(2W)#3	2.80(2)		2.83(3)
O(1W)−O(3W)		2.66(3)	
O(2W)−O(3W)#4		2.78(3)	
O(2W)#1−O(1W)−O(2W)	81.5(6)		82.1(7)
O(3W)−O(1W)−O(2W)		78.9(8)	
O(2W)#3−O(2W)−O(1W)	89.8(5)		92.5(6)
O(1W)−O(2W)−O(3W)#4		82.4(9)	
O(1W)−O(3W)−O(2W)#4		88.9(8)	

[a] Symmetry transformations used to generate equivalent atoms: #1, x, $-y+1$, z; #3, $-x+1$, y, $-z+1$; #4, $2-x$, $1-y$, $1-z$.

$C_6H_4\cdot 4H_2O$[37] the $(H_2O)_6$ clusters are bonded to others with an analog or boat conformation to form water sheets, and in DAN·$2.5H_2O$ (DAN = 2,4-dimethyl-5-aminobenzo[b]-1,8-naphthyridine)[38] the clusters are bonded through hydrogen bonds to form chains in which 4- and 6-membered rings are fused.

Finally, there are "$(H_2O)_6$" clusters like those present in $[Pr(pdc)(pdcH)2H_2O]\cdot 0.4H_2O$[39] ($H_2pdc$ = pyridine-2,6-dicarboxylic acid) and $[Zn(H_2biim)_2(OH_2)_2(ina)_2]\cdot 4H_2O$[40] ($H_2biim$ = 2,2′-biimidazole; ina = isonicotinate) where the water molecules are coordinated to the metal atom and are not free. Another interesting example is found in $[CuL(O_2C-CH_2-C_6H_4-pOH)]\cdot 2H_2O$ (H_3L = *N*,*N*′-1,3-diylbis(salicyldiimino)propan-2-ol)]·$2H_2O$,[41] where the "$(H_2O)_6$" ring is actually formed by two OH groups and by four water molecules.

[(AuPEt$_3$)$_2$-o-hpspa] (5). The crystal is monoclinic, space group $P2(1)/n$, and contains $[(AuPEt_3)_2$-o-hpspa] units involved in a network of hydrogen bonds. The structure and the numbering scheme are shown in Figure 6 and significant structural parameters are listed in Table 5.

In each $[(AuPEt_3)_2$-o-hpspa] unit there are two Au atoms, Au(1) and Au(2), with different coordinative environments. Au(2) is bonded to the S atom of the deprotonated sulfanyl group and to the P atom of PEt_3, while Au(1) is also coordinated to one O atom of the carboxylate group [Au−O (2.585(5)Å)]. This distance is significantly less than the sum

(37) Rodríguez-Cuamatri, P.; Vargas-Diaz, G.; Höpfl, H. *Angew. Chem., Int. Ed.* **2004**, *43*, 3041.
(38) Custelcean, R.; Afloroaei, C.; Vlassa, M.; Polverejan, M. *Angew. Chem., Int. Ed.* **2000**, *39*, 3094.
(39) Ghosh, S. K.; Bharadwaj, P. K. *Inorg. Chem.* **2003**, *42*, 8250.
(40) Ye, B.-H.; Ding, B.-B.; Weng, J.-Q.; Chen, X.-M. *Inorg. Chem.* **2004**, *43*, 6866.
(41) Mukherjee, A.; Saha, M. K.; Nethaji, M.; Chakravarty, A. R. *New J. Chem.* **2005**, *29*, 596.

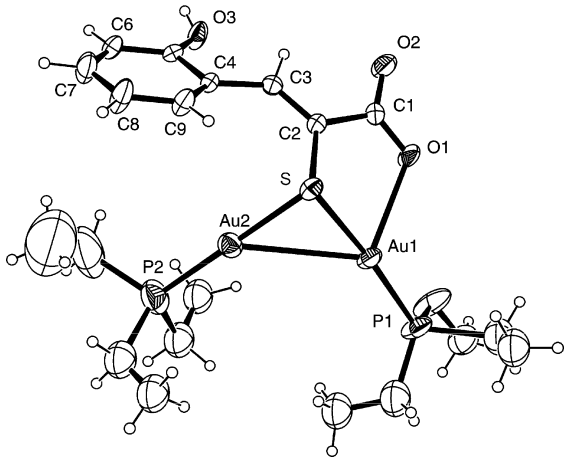

Figure 6. Molecular structure of [(AuPEt$_3$)$_2$-o-hpspa] showing the numbering scheme.

Table 5. Selected Bond Lengths (Å) and Angles (°) in [(AuPEt$_3$)$_2$-o-hpspa] (**5**)

	(a) Au Environment		
Au(1)−P(1)	2.242(3)	P(1)−Au(1)−S	174.24(8)
Au(1)−S	2.363(2)	P(1)−Au(1)−O(1)	111.71(14)
Au(1)−Au(2)	3.1677(5)	S−Au(1)−O(1)	74.05(14)
Au(1)−O(1)	2.585(5)	P(1)−Au(1)−Au(2)	128.83(8)
		S−Au(1)−Au(2)	47.24(5)
		C(2)−S−Au(1)	103.1(3)
		C(11)−P(1)−Au(1)	111.1(4)
		C(13A)−P(1)−Au(1)	111.4(7)
		C(15B)−P(1)−Au(1)	109.1(8)
		O(1)−Au(1)−Au(2)	107.39(13)
		C(1)−O(1)−Au(1)	116.3(5)
Au(2)−S	2.335(2)	P(2)−Au(2)−S	179.82(11)
Au(2)−P(2)	2.246(3)	P(2)−Au(2)−Au(1)	132.16(10)
		S−Au(2)−Au(1)	47.99(5)
		C(2)−S−Au(2)	108.5(2)
		C(23B)−P(2)−Au(2)	121.0(10)
		C(21B)−P(2)−Au(2)	110.1(9)
		C(25)−P(2)−Au(2)	112.4(7)
		C(21A)−P(2)−Au(2)	112.4(7)
		C(23A)−P(2)−Au(2)	116.1(6)
	(b) o-hpspa		
S−C(2)	1.774(7)	O(2)−C(1)−O(1)	123.9(8)
O(1)−C(1)	1.241(9)	O(2)−C(1)−C(2)	118.1(8)
O(2)−C(1)	1.227(9)	O(1)−C(1)−C(2)	118.0(7)
O(3)−C(5)	1.337(9)	C(1)−C(2)−S	117.1(6)
C(1)−C(2)	1.524(10)	C(3)−C(2)−C(1)	118.0(7)
C(2)−C(3)	1.353(10)	C(3)−C(2)−S	124.9(6)
C(3)−C(4)	1.456(10)	C(4)−C(9)−C(8)	121.5(8)
		C(2)−C(3)−C(4)	133.0(7)

of the van der Walls radii (3.20 Å),[28] less than the Au−O bond distances previously described in this paper, and similar to those found in complexes of type [(AuPPh$_3$)$_2$xspa] with similar ligands.[17] This interaction has a significant effect on the structural parameters of the metal environment. The parameter that is most markedly affected by the Au−O interaction is the S−Au−P angle, which is 174.24(8)° for Au(1) and 179.82(11)° for Au(2). The Au····Au [3.1677(5) Å] distance is less than the sum of the van der Walls radii for gold (3.70 Å)[28] and also less than the intramolecular Au···Au distances found in the previous structures.

The structural features of this unit are in contrast with the cases discussed previously, and they resemble those found in the [(AuPPh$_3$)$_2$xspa] compounds already described.[17] The main difference between the structures of **1**·3H$_2$O, **6**·3H$_2$O, and **9**·3H$_2$O and this one in terms of the Au unit is the coordination of the carboxylate group and the formation of dimers.

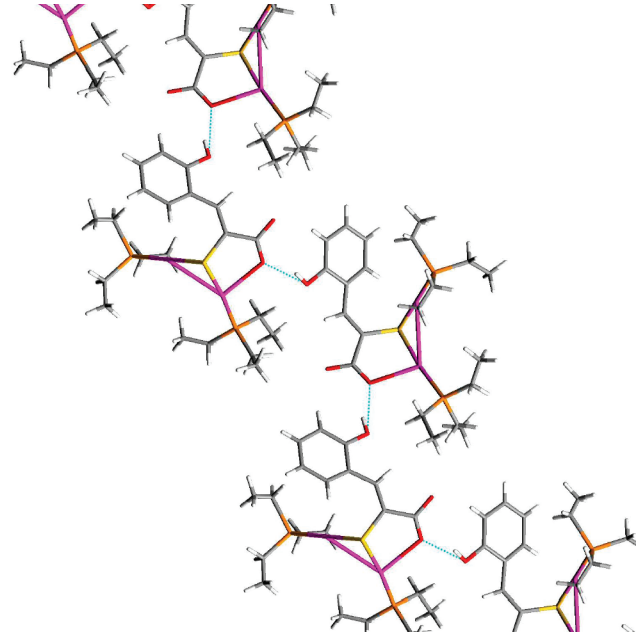

Figure 7. Hydrogen bonding interactions in [(AuPEt$_3$)$_2$-o-hpspa].

When the O atom of the carboxylate group acts as a bridge between two Au atoms (**1**·3H$_2$O, **6**·3H$_2$O, and **9**·3H$_2$O) the ligands are planar, or essentially planar, but in **5** the CSCOO fragment is not planar [SC(2)C(1)O(1) torsion angle: 18.5(10)°] and the phenyl ring deviates significantly from the C(3)C(2)C(1)S plane [C(9)C(4)C(3)C(2) torsion angle: 3.8(13)°]. This spatial arrangement allows, or is the result of, the O−H···O interaction present in the crystal, where hydrogen bonds exist between the O(3)−H(3) group of the phenyl ring and the O(1) atom of the carboxylate group of a neighboring molecule [O(3)−H(3)···O(1)#1 0.73(9), 1.82(9), 2.529(8 Å, 163(10)°], thus leading to a polymeric structure (see Figure 7).

IR Spectroscopy. Comparison of the spectra of these compounds with those of the free H$_2$L ligands shows the disappearance of the ν(SH) band (at about 2590−2560 cm^{-1}) and the replacement of the CO$_2$H bands (at about 1730−1680 and 1320−1210 cm^{-1}) by bands typical of a carboxylate group. Both of these observations are consistent with bideprotonation of the ligand.

With respect to the carboxylate bands in the complexes, ν_{as}(COO) and ν_{sym}(COO) are close to the positions of these bands in the IR spectra of the sodium salt of the ligands {for example 1574, 1576 and 1566 cm^{-1} [ν_{as}(COO)] and 1383, 1373, and 1392 cm^{-1} [ν_{sym}(COO)] for H$_2$pspa, H$_2$fspa and H$_2$tspa, respectively} and the value of the parameter [ν_{as}(COO) − ν_{sym}(COO)] is low compared[42] with that of a monodentate group. This suggests that in the solid the Au−O interaction is very weak. Note that the situation in the solids of **1**, **6**, and **9** could be different to those found by X-ray

(42) Nakamoto, K. *Infrared and Raman Spectra of Inorganic and Coordination Compounds*, 5th Ed.; John Wiley: New York, 1997; part B, p 60.

crystallography, as could also be the case (vide infra) for **5**, as the crystals were obtained from a dmso-d_6 solution and the solid from methanol/water.

NMR Spectroscopy. The main modifications in the ^{1}H NMR spectra of the H_2L ligands upon formation of the complexes are the disappearance of the C(2)SH (at about 5 ppm) and the CO_2H (at about 13 ppm) signals. This is consistent with deprotonation of both groups. Another common characteristic of all the spectra, except those of H_2cpa and H_2fspa in $CDCl_3$ and H_2-o-pyspa derivatives, is the shift to higher field of the C(3)H signal with respect to that in the free ligand, suggesting that the S-coordination found in the solid state, as in other complexes of these ligands, remains in solution.[17,43,44] In addition, all the spectra show signals due to the PEt_3 groups and these are located around 1.10 and 1.80 ppm for CH_3 and CH_2, respectively

The spectrum of the [$(AuPEt_3)_2$-o-pyspa] complex does not show the signal due to the NH group, which is present in the spectrum of the free ligand, and this reflects deprotonation of this group and the evolution of the ligand to the thiol form, with the subsequent coordination of the metal to this group.

In the ^{13}C NMR spectra the signals are shifted with respect to those of the free ligands because of the coordination to the metal atom. For [$(AuPEt_3)_2$-o-pyspa], the C(2) signal is significantly shielded and C(3) is deshielded because of the evolution of the ligand to the thiol form and subsequent coordination to the Au atom.

The C(1) signal for the pspa, fspa, and tspa complexes in the dmso-d_6 spectra is close to those found in complexes of the type [$(AuPPh_3)_2$L] with equivalent ligands;[17] in the latter compounds the coordination mode of L is similar to that found for L in **5**. The isolation of this complex from a dmso-d_6 solution and the position of the C(1) signal in the spectra of the other complexes suggest[45,46] the possibility of a similar coordinative mode in this solvent in all of these cases.

The ^{31}P NMR spectra consist of one singlet located at around 39 ppm, attributed to the coordinated PEt_3, and this is close to the signal found in other complexes with S−Au−PEt_3 fragments.[47–50] The ^{13}C and ^{31}P{1H} chemical shifts and ^{31}P{1H}-^{13}C coupling constants are consistent with compounds of this type.[50] Some spectra show the presence of a very weak signal at around 54 ppm and this can be attributed to $OPEt_3$.[48] A peak at around −18.6 ppm that could be assigned to PEt_3 was not observed.[49,51]

To investigate the formation of $OPEt_3$ we followed the evolution of the ^{31}P NMR spectrum of **9** using dmso-d_6 as solvent. The ^{31}P spectrum of a recently prepared solution of **9** shows only a signal at 39.1 ppm attributable to [$(AuPEt_3)_2$tspa]. After 20 min a second signal appears at 54.7 ppm, in this case attributable to $OPEt_3$. The amounts of the different species after 45 min, estimated from the integrated peaks, are [$(AuPEt_3)_2$tspa] 98.5% and $OPEt_3$ 1.5%. After 55 days, the 39.1 ppm signal remained and a new weak signal at 39.5 ppm was identified. This latter signal could be attributed to the PEt_3 coordinated in [$(AuPEt_3)$(Htspa)], with both species representing about 67%. The $OPEt_3$ signal remained and this species represented about 10.8%. A new signal at 51.1 ppm was seen and this was assigned to $[Au(PEt_3)_2]^{+}$[48] (about 22.4%), an ion also present in the MS(FAB) spectra.

During the experiment a signal attributable to the free PEt_3 was not observed, meaning that the oxidation of this species is rapid; however, **9** showed a slow rate of decomposition.

Antiinflammatory Activity. The antiinflammatory effect of the compounds at doses of 2.5 and 5 mg/Kg are shown in Table 6 and are compared with the control. As can be seen, the complexes, except **11**, are active at a dose of 5 mg/Kg. The activities are higher than those of the ligands (for example, H_2pspa, H_2fspa, and H_2tspa, at a dose of 5 mg/Kg showed percentages of inflammation of 19.60, 39.25, 7.51% and reduction of 40.10, −19.77, 77.02%, respectively), which is in contrast with previous results on Zn-metalation of pyrazolones[52] and underlines the positive effect of the metal.

Despite these findings, the influence of the ligand on the activity of the complexes is evident. On comparing the activities of the complexes that contain the phenyl, furan, thiophene, or pyridine ring it can be seen that the best result is obtained for the thiophene derivative (**9**) and the worst for the pyridine derivative (**10**); however, the introduction of substituents on the phenyl ring changes the activity, with hydroxy and chloro substituents in the ortho-position being the most effective. The additional incorporation of Br atoms into the o-hydroxyphenyl derivative decreases the activity.

The values of the inflammation reduction for the best compounds are higher than those of $AuPEt_3Cl$ and also higher than those previously found in other compounds of Au(I), Au(III), and auranofin in this induced edema.[53,54] To make comparisons with other agents, indomethacin, an antiinflammatory used as a positive test in studies carried out under the same conditions,[55,56] shows a percentage of inflammation reduction of 35.87% at the 5 mg/Kg level.

The high antinflammatory activity of some of these compounds, together with the recent positive data on a combination therapy for rheumatoid arthritis that includes

(43) Casas, J. S.; Castiñeiras, A.; Couce, M. D.; Jorge, M. L.; Russo, U.; Sánchez, A.; Seoane, R.; Sordo, J.; Varela, J. M. *Appl. Organomet. Chem.* **2000**, *14*, 421.
(44) Casas, J. S.; Castiñeiras, A.; Couce, M. D.; Playá, N.; Russo, U.; Sánchez, A.; Sordo, J.; Varela, J. M. *J. Chem. Soc., Dalton Trans.* **1998**, 1513.
(45) Gajda-Schrantz, K.; Nagy, L.; Kuzmann, E.; Vertes, A.; Holecek, J.; Lycka, A. *J. Chem. Soc., Dalton Trans.* **1997**, 2201.
(46) Holecek, J.; Lycka, A.; Nadvornik, M.; Handlir, K. *Collect. Czech. Chem. Commun.* **1991**, *56*, 1908.
(47) Coffer, M. T.; Shaw, C. F., III; Eidsness, M. K.; Watkins II, J. W.; Elder, R. C. *Inorg. Chem.* **1986**, *25*, 333.
(48) Isab, A. A.; Hormann, A. L.; Coffer, M. T.; Shaw, C. F., III *J. Am. Chem. Soc.* **1988**, *110*, 3278.
(49) Ahmad, S.; Isab, A. A. *J. Inorg. Biochem.* **2002**, *88*, 44.
(50) Kang, J. G.; Cho, H. K.; Park, C.; Yun, S. S.; Kim, J. K.; Broker, G. A.; Smyth, D. R.; Tiekink, E. R. T. *Inorg. Chem.* **2007**, *46*, 8228.
(51) Isab, A. A.; Hussain, M. S.; Katar, M. N.; Wazeer, M. I. M.; Al-Arfaj, A. R. *Polyhedron* **1999**, *18*, 1401.
(52) Casas, J. S.; Castaño, M. V.; Castellano, M. E. E.; Ellena, J.; García-Tasende, M. S.; Gato, A.; Sánchez, A.; Sanjuan, L. M.; Sordo, J. *Inorg. Chem.* **2002**, *41*, 1550.
(53) Coppi, G.; Borella, F.; Gatti, M. T.; Comini, A.; Dall'Asta, L. *Boll. Chim. Farm.* **1989**, *128*, 22.
(54) Girard, G. G.; Hill, D. T.; Dimartino, M. J. *Inorg. Chim. Acta* **1989**, *166*, 141.

Table 6. Anti-inflammatory Effect of the Compounds Tested against Plantar Edema Induced by Carrageenan

compound	dose(mg/Kg)	animals	% inflammation	% reduction
control		12	32.77 ± 1.89	
[$(AuPEt_3)_2$pspa] (**1**)	2.5	9	17.33 ± 1.70[a]	47.11 ± 5.3
	5	9	3.60 ± 0.80[a]	88.78 ± 2.6
[$(AuPEt_3)_2$Clpspa] (**2**)	2.5	9	8.01 ± 1.40[a]	75.5 ± 4.40
	5	9	2.36 ± 0.60[a]	92.85 ± 2.06
[$(AuPEt_3)_2$-o-mpspa] (**3**)	2.5	9	33.3 ± 2.06	−1.90 ± 6.20
	5	9	16.64 ± 2.10[a]	49.18 ± 6.40
[$(AuPEt_3)_2$-p-mpspa] (**4**)	2.5	9	24.05 ± 1.5[a]	26.56 ± 4.8
	5	9	19.12 ± 2.7[a]	41.65 ± 8.4
[$(AuPEt_3)_2$-o-hpspa] (**5**)	2.5	9	6.04 ± 1.72[a]	81.54 ± 5.25
	5	9	−0.08 ± 1.90[a]	100.24 ± 5.80
[$(AuPEt_3)_2$-p-hpspa] (**6**)	2.5	9	20.72 ± 0.81[a]	36.74 ± 2.48
	5	9	9.99 ± 1.05[a]	69.48 ± 3.22
[$(AuPEt_3)_2$-diBr-o-hpspa] (**7**)	2.5	9	25.53 ± 1.8[a]	22.06 ± 5.4
	5	9	20.25 ± 3.3[a]	38.16 ± 10.2
[$(AuPEt_3)_2$fspa] (**8**)	2.5	9	16.86 ± 1.66[a]	48.54 ± 5.08
	5	9	2.10 ± 2.22[a]	93.56 ± 1.54
[$(AuPEt_3)_2$tspa] (**9**)	2.5	8	4.84 ± 1.65[a]	85.15 ± 5.04
	5	8	1.10 ± 1.37[a]	96.61 ± 4.19
[$(AuPEt_3)_2$-o-pyspa] (**10**)	2.5	9	17.40 ± 1.08[a]	46.86 ± 3.3
	5	9	12.70 ± 1.0[a]	61.22 ± 4.0
[$(AuPEt_3)_2$cpa] (**11**)	2.5	9	40.29 ± 1.7	−2.30 ± 2.60
	5	9	48.7 ± 1.8	−2.78 ± 2.80
$AuPEt_3Cl$	2.5	9	13.23 ± 1.39[a]	59.5 ± 4.2
	5	9	12.40 ± 1.4[a]	62.13 ± 4.4

[a] Significant with respect to the control ($P \leq 0.05$).

gold compounds,[57] warrants additional testing of the activity against this illness for the active compounds.

Conclusions

The synthesis and the structural study of complexes of the type [$(AuPEt_3)_2$xspa] [where H_2xspa = R—CH═C(SH)—COOH] enabled the identification of two classes of structures. One of them consists of [$(AuPEt_3)_2$xspa]$_2$ dimers, a tetranuclear unit that contains an Au_4 ring, and these are hydrogen bonded to $(H_2O)_6$ clusters. In the other system the dinuclear motif [$(AuPEt_3)_2$xspa] does not dimerize.

The first class of compounds gives the opportunity to visualize a structural motif present in the oxidation products of Au(I) phosphine thiolate compounds such as auranofin and at the same time, because of the use of different R groups in the precursor acids, enables us to analyze the influence of different chemical environments on the $(H_2O)_6$ cluster parameters.

The antiinflammatory activities of the compounds prepared show that, in general, all of them are active but that the influence of the R substituents on the antiinflammatory activity is significant, with the o-hpspa and the tspa derivatives being the most active.

Acknowledgment. We thank the Spanish Ministry of Science and Technology for financial support under projects BQU2002-04524-CO2-01 and BQU2002-04524-CO2-02, and the Xunta the Galicia, Spain, for support under projects PGIDIT03PXIC20306PN and PGIDIT03PXIC30103PN.

Supporting Information Available: Figures S1, S2 containing crystal structure of [$(AuPEt_3)_2$-p-hpspa]$_2$ in **6**·3H_2O and of [$(AuPEt_3)_2$tspa]$_2$ in **9**·3H_2O (PDF). This material is available free of charge via the Internet at http://pubs.acs.org. Also, crystallographic data for this paper can be obtained at the Cambridge Crystallographic Data Centre [CCDC numbers 676684, 676685, 676686 and 676687 for **1**·3H_2O, **5**, **6**·3H_2O and **9**·3H_2O respectively].

IC800314P

(55) Guzmán, S.; Gato, A.; Calleja, J. M. *Phyther. Res.* **2001**, *15*, 224.
(56) Guzmán, S.; Gato, A.; Lamela, M.; Freire-Garabad, M.; Calleja, J. M. *Phyther. Res.* **2003**, *17*, 665.
(57) Lehman, A. J.; Esdaile, J. M.; Klinkhoff, A. V.; Grant, E.; Fitzgerald, A.; Canvin, J. *Arthritis Rheum.* **2005**, *52*, 1360.